Supplementary Information

The integration of social influence and reward: computational approaches and neural evidence

Damon Tomlin[a], Andrea Nedic[b], Deborah A. Prentice[c], Philip Holmes[d, e, f], and Jonathan

D. Cohen[c, d]

a. Department of Psychology
University of Colorado, Colorado Springs
Colorado Springs, Colorado, USA

b. Princeton Consultants
New York, New York, USA

c. Department of Psychology
Princeton University
Princeton, New Jersey, USA

d. Princeton Neuroscience Institute
Princeton University
Princeton, New Jersey, USA

e. Department of Mechanical and Aerospace Engineering
Princeton University
Princeton, New Jersey, USA

f. Program in Applied and Computational Mathematics
Princeton University
Princeton, New Jersey, USA
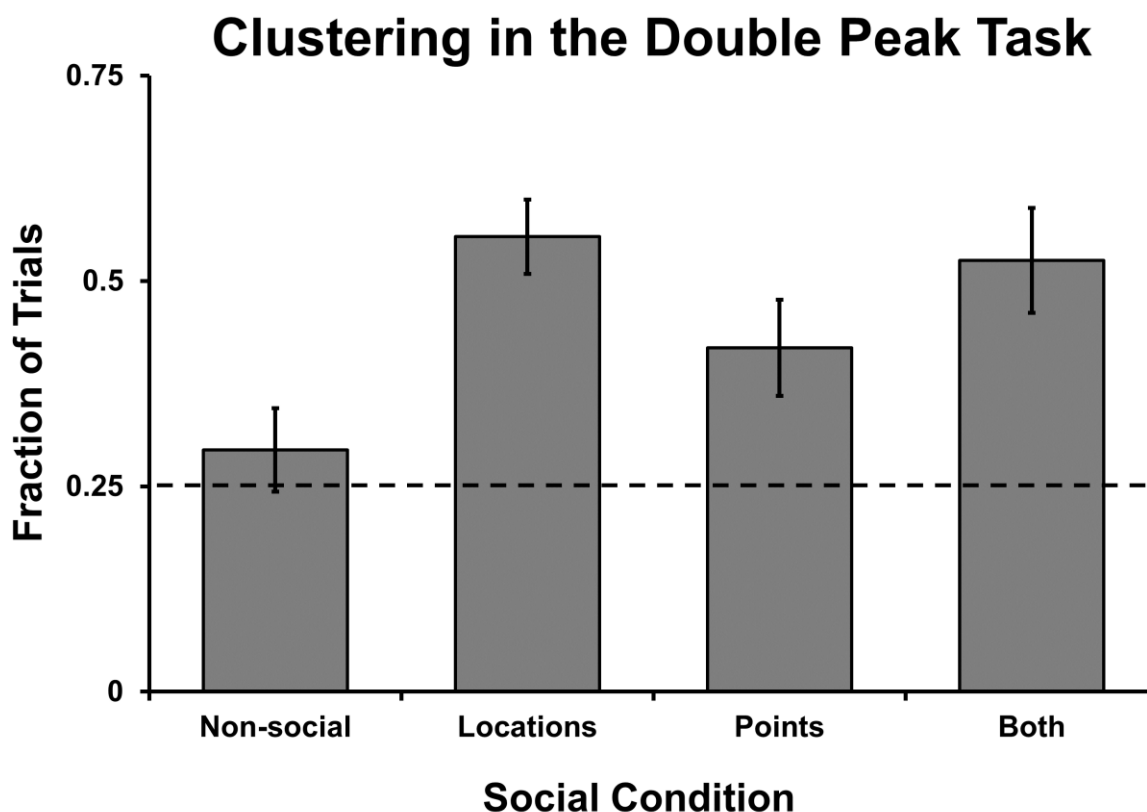
**Figure S1. Clustering in the Double Peak task.**

In order to examine the impact of social information, the Double Peak task contained two equally profitable locations along the relevant dimension. If groups of participants were to choose their preferred locations at random, the probability that all three members of the group would lie on the same side of the midline would be 25%. However, if participants tended to choose one peak over the other based upon the locations of other group members, this probability would be significantly higher. Figure S3 indicates the frequency with which group members were so co-localized. Analysis revealed that the probability that all three participants were on the same side of the midline was significantly higher than 25% for the Locations, Points, and Both conditions ($p < 10^{-5}$, $p < .03$, and $p < 10^{-3}$, respectively; corrected for multiple comparisons), but not the Isolated condition ($p > 1.0$, corrected for multiple comparisons). In addition, an ANOVA revealed that the frequency of clustering was higher for the Locations and Both conditions than the Isolated condition ($p < .01$ and $p < .05$, respectively); all other comparisons were not statistically significant. The significance of clustering under the Points condition most likely indicates a group tendency to remain on the first peak encountered (especially when the participant's earnings were visible).
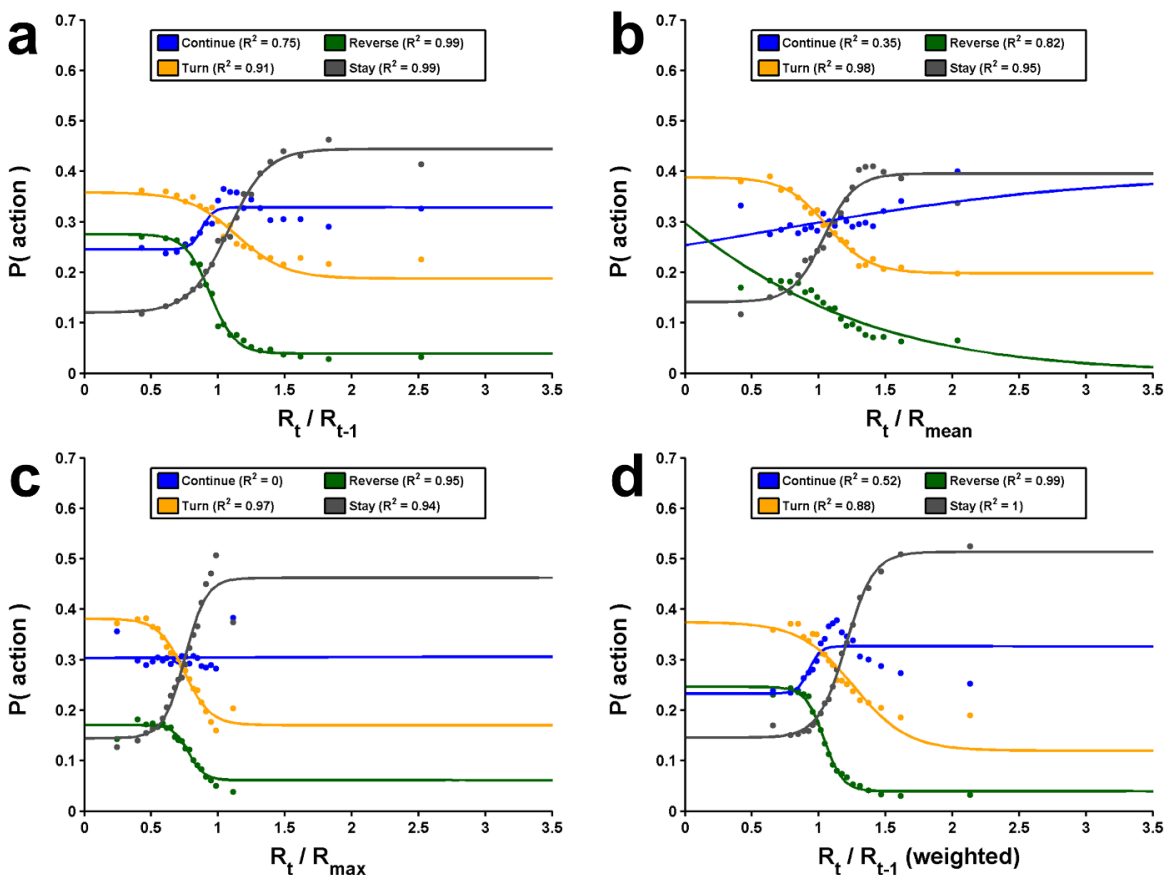
Figure S2. Decomposition of reward-based action probabilities

Reward-based action probabilities, across all participants and social conditions, for each of the four action types as a function of four possible input variables: (**A**) the ratio of current earnings to most recent earnings (the metric used in the main text; $SS_{residual}$ = .0173). (**B**) the ratio of current earnings to the mean earnings experienced at that point in the block ($SS_{residual}$ = .0268). (**C**) the ratio of current earnings to the maximum single-trial earnings previously experienced in the block ($SS_{residual}$ = .0309). (**D**) the exponentially weighted ratios of current earnings to previous earnings across all previous trials in the block ($SS_{residual}$ = .0319). Trials were sorted into bins according to the aforementioned metrics and action type; probabilities were estimated by calculating the number of choices corresponding to each action type for each bin. The goodness of fits are indicated by R^2 values for each action type. The simple reward ratio depicted in (**A**) provided the best fit to the data (i.e., the minimum $SS_{residual}$). While results are shown for 20 bins, the identity of the best metric did not depend crucially on the number of bins used. Consistent with our modeling of individual participants, *continuing* and *staying* were more likely when reward ratios were high, while *reversing* and *turning* were more likely when reward ratios were low. Action probabilities provided a close approximation to logistic functions, which were then used to model reward-based decisions.
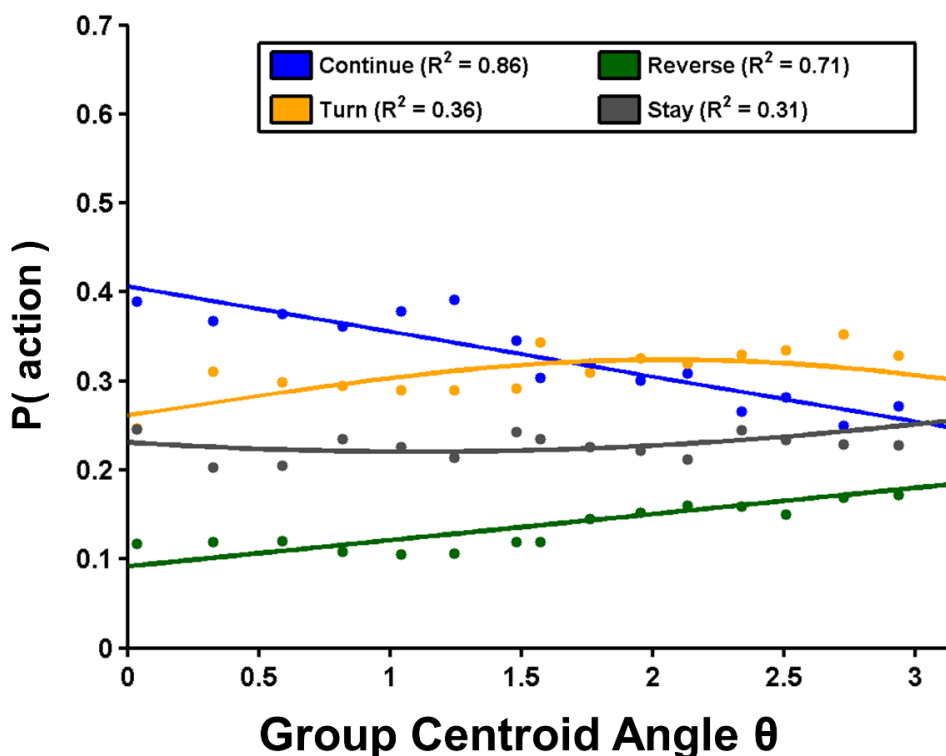
Figure S3. Socially-based action probabilities.

Socially-based action probabilities, across all participants, for each of the four action types as a function of θ: the angle between the participant's direction of travel and the centroid of the group. Data were pooled across all decisions in the Locations and Both conditions, then sorted into bins according to θ and action type. Probabilities were then estimated by calculating the number of decisions corresponding to each action type within each bin. Consistent with our modeling at the level of individual participants, participants were more likely to continue when θ was small (i.e., the group centroid was ahead of the participant), and were more likely to reverse when θ was large (i.e., the group centroid was behind the participant). Because θ described an angle, and therefore existed along a continuous circle around the participant, sine functions were used to model socially-based decisions. Note that the probability functions displayed above do not account for the separate effect of reward-based information.

Effect of Finding the Global Maximum on the Valley Task
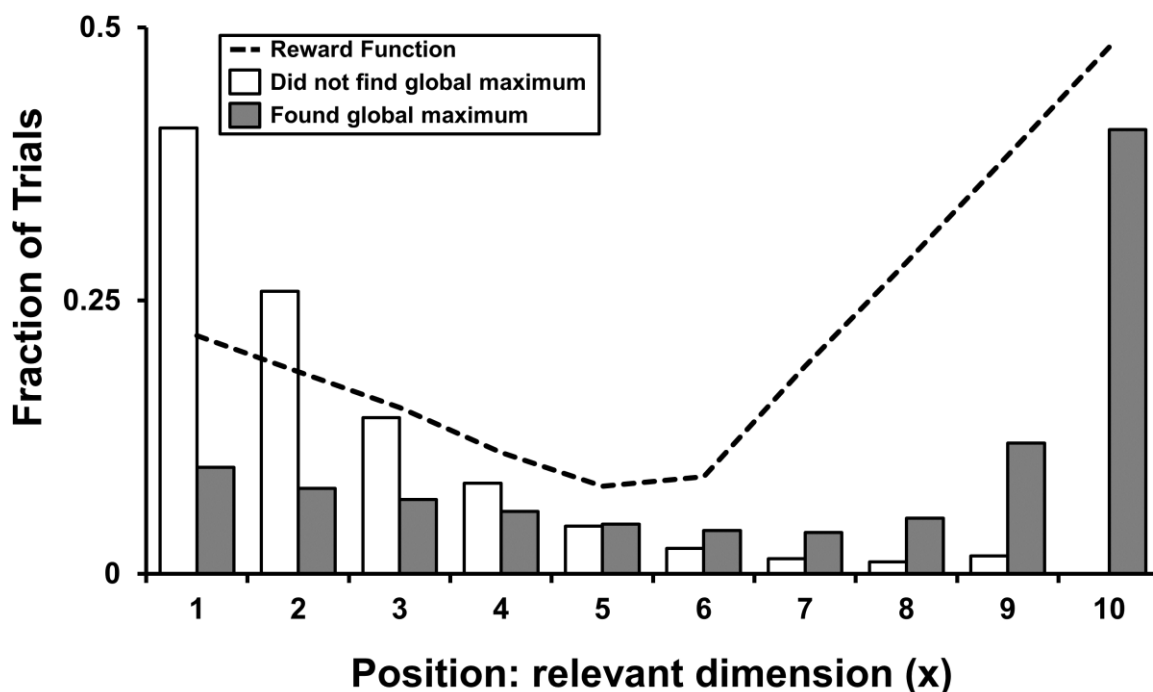
Figure S4. Effect of finding the global maximum in the Valley task.

Analysis indicated that 56% of participants reached the global maximum in the Valley task (pooled across social conditions). Participants that did not find the global maximum spent 41% of trials at the local maximum (left side of graph), while those that did find the global maximum spent 41% of trials at the global maximum (right side of graph). Thus, participants predicated subsequent behavior upon the rewards they earned during the task.
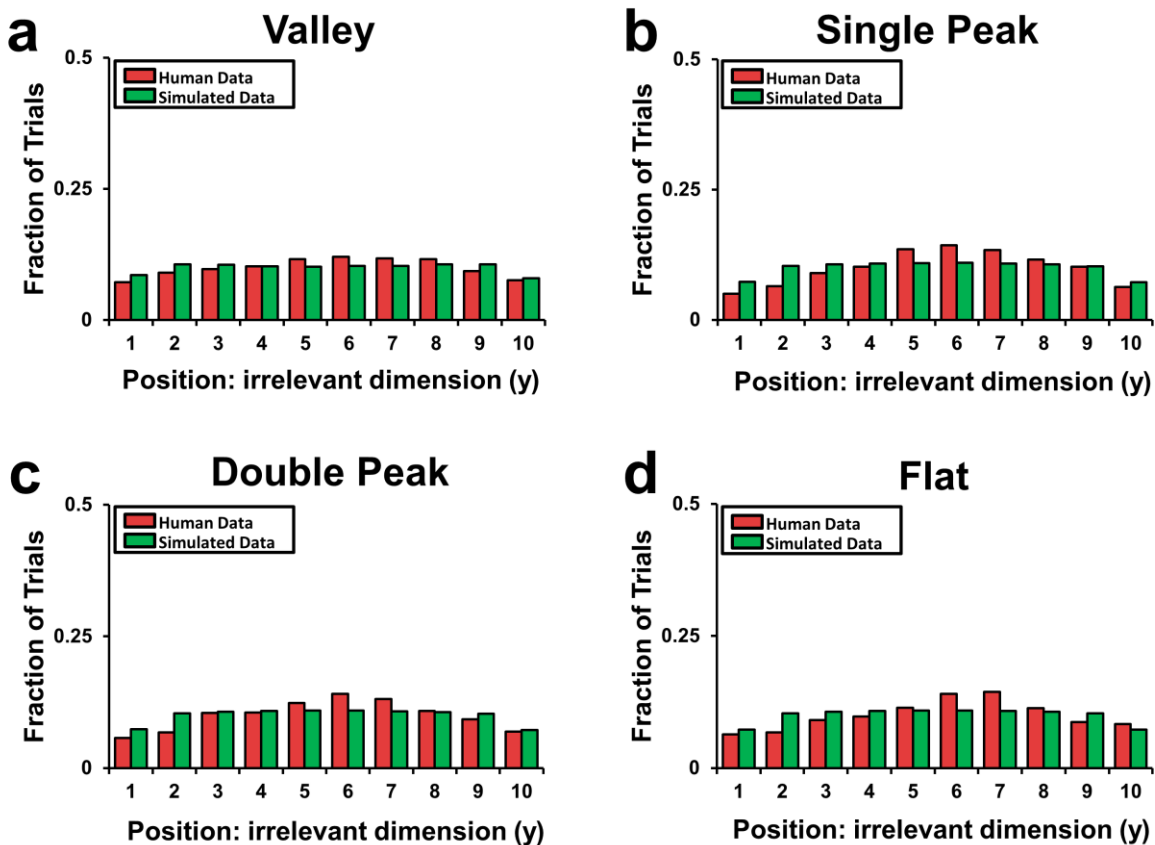
Figure S5. Distributions along the irrelevant dimension

Red bars indicate the fraction of trials (y axis) that were spent by human participants at a given location (x axis) along the irrelevant dimension; green bars indicate the fraction of trials spent by simulated agents at the same location. Although results were similar across all four tasks, data are shown separately for each.

Perseveration-based Action Probabilities
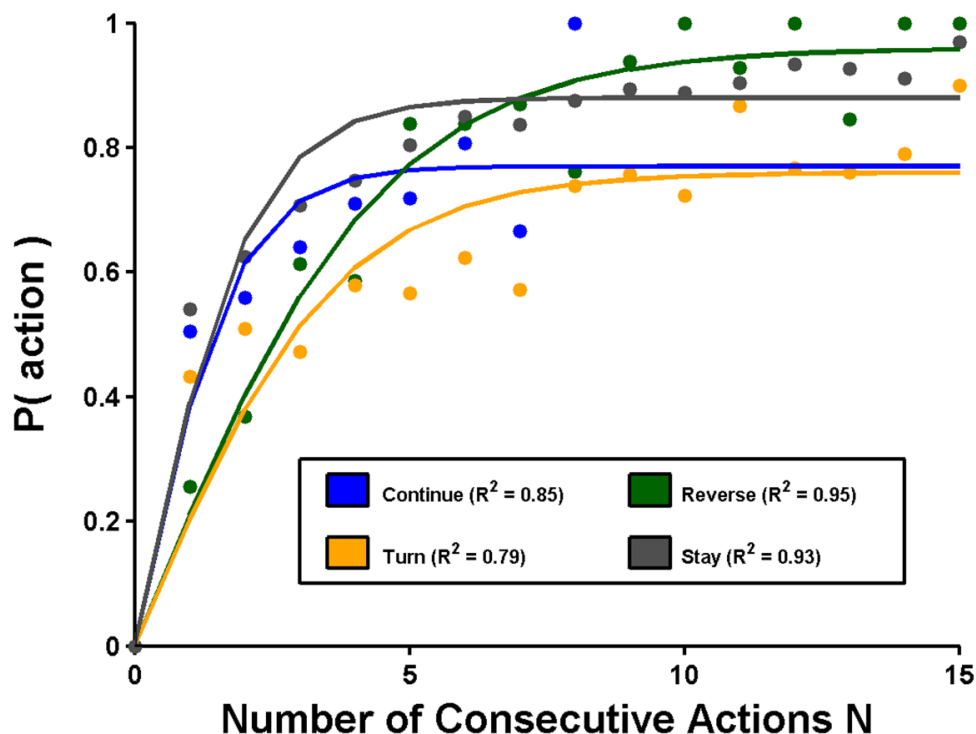
**Figure S6. Perseveration sorted by action type.**

In order to simplify the model described in the main text, a single function describing perseveration behavior was applied to all four action types. While this simplification would be inappropriate if perseveration behavior varied between the action types, the data above show a similar pattern for each action type. Data were pooled across participants and sorted according to how many actions of a given type had been consecutively repeated. Probabilities were then calculated according to the frequency with which the action type of a given decision matched the action type that had been previously repeated. Note that the probability functions displayed above are averages across all decisions, and do not account for the effect of reward-based or socially-based information.

Akaike Information Criterion Values across Models
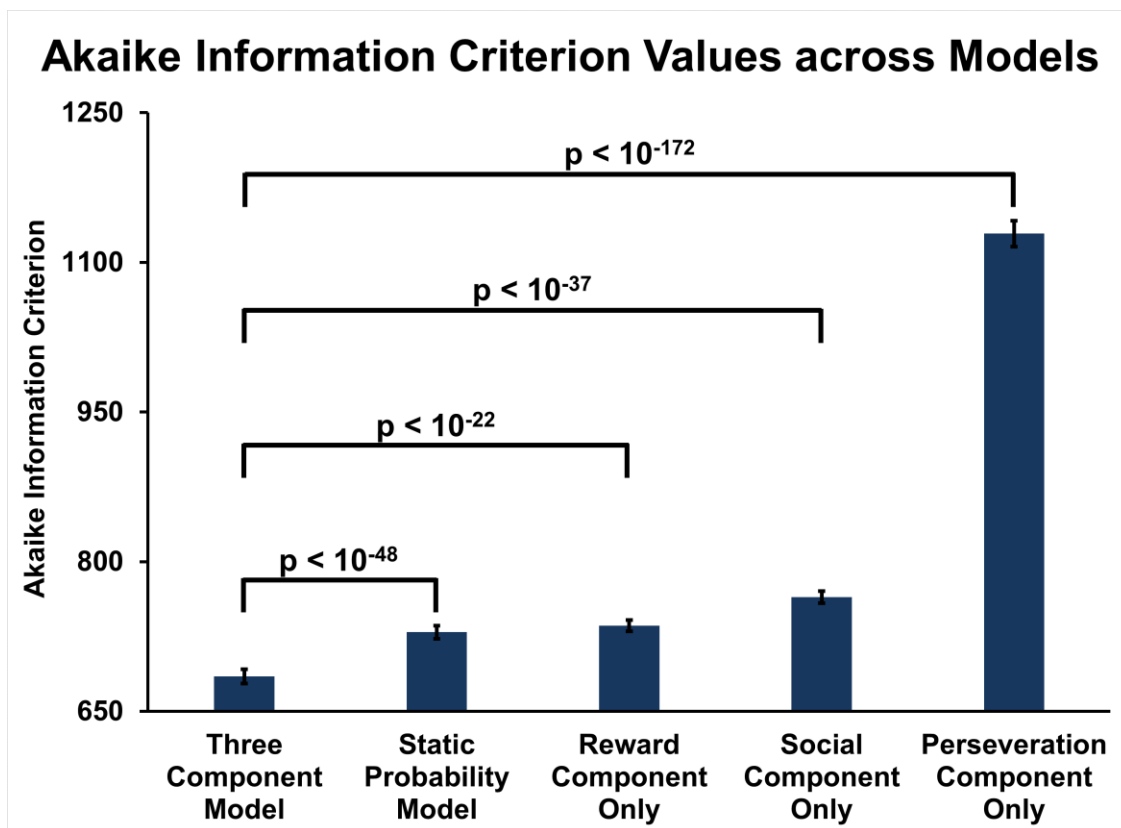
Figure S7. Comparison of alternative models.

In order to verify that the three-component model detailed in the main text was the best explanation of the data, it was compared to four alternative models. The quality of all models was assessed using the Akaike Information Criterion (AIC), which weighs the explanatory power of a model against the number of free parameters that the model employs (lower values of the criterion indicate a better fit after the number of parameters is taken into account). The first alternative model, labeled as the "probabilistic" model, had the same three components as the model described in the main text but was not sensitive to context: instead of the functions depicted in Figures 5 and 6, static probabilities were fit to each action type (for the reward-based and socially-based components) and a single probability was fit to the participant's perseveration component. Thus, while the three-component model described in the main text employed 27 parameters (mean AIC: 717.1; SD: 130.1), the probabilistic model depended on only 8 (mean AIC: 729.3; SD: 119.0). The other alternative models were the isolated components of the three-component model: reward-based (12 parameters; mean AIC: 736.0; SD: 102.3), socially-based (12 parameters; mean AIC: 764.4; SD: 108.5), and perseveration-based (2 parameters; mean AIC: 1128.9; SD: 233.4). However, even after accounting for these differences in the number of parameters, the three-component model described in the main text was nevertheless significantly better than these alternatives when AIC values were compared across participants (p-values for paired t-tests are depicted above).

a

BOLD response ∝ reward ratio R

Y = 6 mm   Z = -7 mm

b

BOLD response ∝ centroid angle θ

Y = -3 mm   Z = 50 mm

c

BOLD response ∝ consecutive actions N

X = -3 mm   Z = -3 mm

corrected p value

10^{-6}
10^{-4}
.01
1
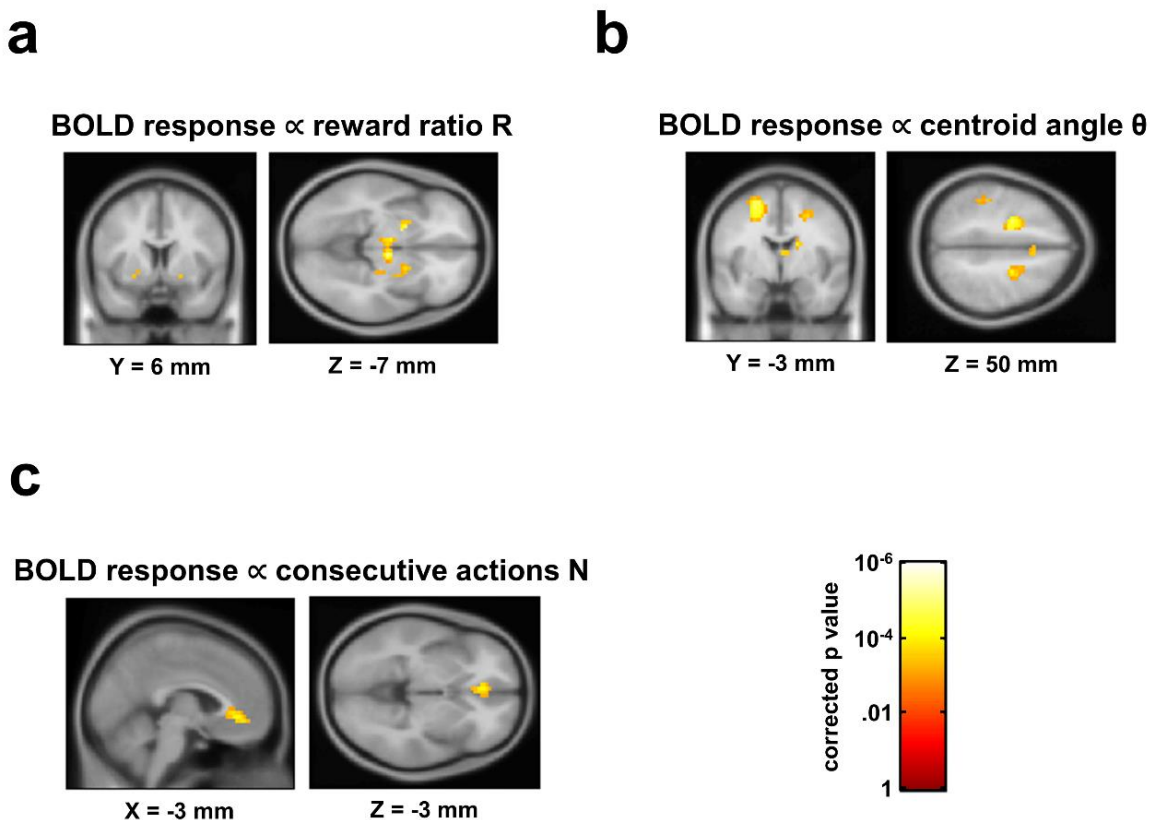
Figure S8. Neural substrates of source inputs.

Neuroimaging analysis revealed several regions whose activity was positively correlated with the inputs to the three components of the proposed model. All images are thresholded at correct p < .001, 5 contiguous voxels. (**A**) Regions whose activity was positively correlated with the input to the reward-based component: the reward ratio R. These regions included the visual cortex, midbrain, and bilateral putamen. (**B**) Regions whose activity was positively correlated with the input to the socially-based component: the group centroid angle θ. These regions include the supplementary motor area and left parietal cortex. (**C**) Regions whose activity was positively correlated with the input the perseveration-based component: the number of consecutively repeated actions, N. In this case, there was a single region: the ventromedial prefrontal cortex.
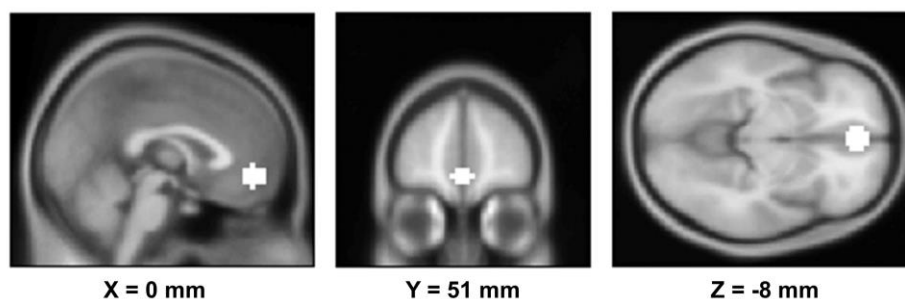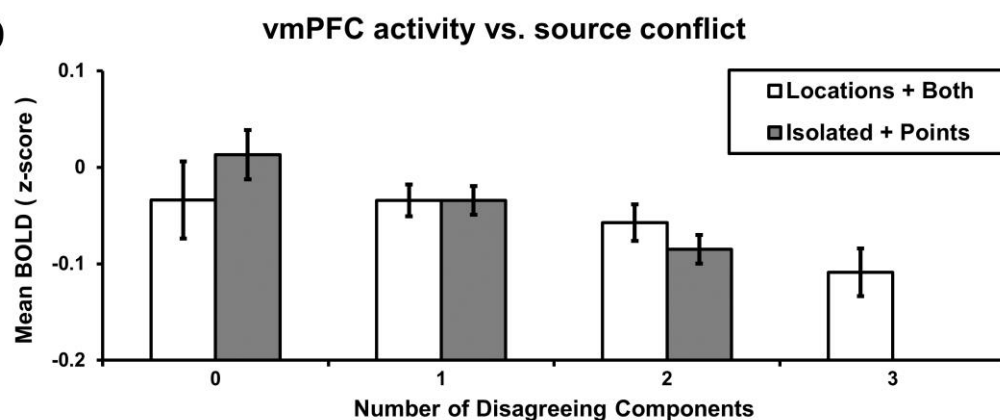
Figure S9. Region-of-interest analysis of the ventromedial prefrontal cortex.

The vmPFC was used as a control region to test the specificity of activity exhibited by the regions shown in Figure 7. (**A**) The vmPFC was defined as a region-of-interest centered at (X = 0 mm; Y = 51 mm; Z = -8 mm), with a radius of 8 mm. (**B**) A joint analysis pooling data for which locations of other group members were available and unavailable revealed no effect of source disagreement, location availability, or interaction (respectively, $F_{2,339} = 2.15$, p = .12; $F_{1,339} = .07$, p = .79; $F_{2,339} = .79$, p = .46). There was also no effect of source disagreement in a separate analysis of trials for which location-based information was available ($F_{3,225} = 5.72$, p = .31). There *was* an effect of source disagreement on trials for which location-based information was unavailable ($F_{2,175} = 5.72$, p < .005, $\omega^2 = .05$); however, the pattern of activity exhibited by the vmPFC *was the opposite to that shown in Figure 7*: vmPFC activity was *lower* for trials in which there was more disagreement between sources, thereby suggesting a different form of processing in this region. See Table S10 for details on statistical comparisons.

Table S1. Statistical data for inter-participant distances.

	Isolated	Locations	Points	Both
Relevant Dimension: Isolated (M = 7.98, SD = 3.43)	N/A	**p ≤ 10^{-4}**	p = .08	**p ≤ 10^{-9}**
Relevant Dimension: Locations (M = 5.98, SD = 3.10)	**p ≤ 10^{-4}**	N/A	p = .13	**p ≤ .01**
Relevant Dimension: Points (M = 6.95, SD = 3.35)	p = .08	p = .13	N/A	**p ≤ 10^{-6}**
Relevant Dimension: Both (M = 4.57, SD = 2.70)	**p ≤ 10^{-9}**	**p ≤. 01**	**p ≤ 10^{-6}**	N/A
Irrelevant Dimension: Isolated (M = 8.28, SD = 1.90)	N/A	**p ≤ .001**	p = .96	**p ≤ 10^{-9}**
Irrelevant Dimension: Locations (M = 6.87, SD = 2.56)	**p ≤ .001**	N/A	**p ≤ .01**	**p ≤ 10^{-3}**
Irrelevant Dimension: Points (M = 8.11, SD = 2.29)	p = .96	**p ≤ .01**	N/A	**p ≤ 10^{-9}**
Irrelevant Dimension: Both (M = 5.50, SD = 2.09)	**p ≤ 10^{-9}**	**p ≤ 10^{-3}**	**p ≤ 10^{-9}**	N/A
Flat Task: Isolated (M = 8.48, SD = 2.26)	N/A	**p ≤ 10^{-6}**	p = .99	p = .28
Flat Task: Locations (M = 5.92, SD = 1.70)	**p ≤ 10^{-6}**	N/A	**p ≤ 10^{-6}**	**p ≤ .01**
Flat Task: Points (M = 8.61, SD = 1.80)	p = .99	**p ≤ 10^{-6}**	N/A	p = .2
Flat Task: Both (M = 7.32, SD = 2.77)	p = .28	**p ≤ .01**	p = .2	N/A

The leftmost column above indicates the mean and standard deviation of the inter-participant distances from Figure 4. Columns two through five indicate the significance of Tukey's tests between the social conditions indicated by the row and column. For the relevant dimension across tasks other than the Flat task, ANOVA revealed a significant effect of social condition ($F_{3,312}$ = 21.88, p < 10^{-12}, ω^2 = .13) and task ($F_{2,312}$ = 38.12, p < 10^{-14}, ω^2 = .16), and a significant interaction between the two factors ($F_{6,312}$ = 2.45, p < .05, ω^2 = .02). For the irrelevant dimension across tasks other than the Flat task, ANOVA revealed a significant effect of social condition ($F_{3,312}$ = 404.4, p < 10^{-15}, ω^2 = .20) and task ($F_{2,312}$ = 33.13, p < .05, ω^2 = .01), but no significant interaction between the two factors ($F_{6,312}$ = 31.54, p = .37). Finally, ANOVA for the Flat task revealed a significant effect of social condition ($F_{3,212}$ = 13.55, p < 10^{-7}, ω^2 = .15).

Table S2. Statistical data for reaction times across decision classes.

	All Sources	Two of Three Sources	Only Reward	Only Social	Only Perseveration	No Sources
All Sources (M = 1.36, SD = .41) (M = 1.26, SD = .30)	N/A	p = .27	p ≤ .001 p ≤ .05	p ≤ 10^{-4}	p ≤ 10^{-4} p ≤ .001	p ≤ 10^{-7} p ≤ 10^{-8}
Two of Three Sources (M = 1.42, SD = .33)	p = .27	N/A	p = .15	p ≤ .05	p ≤ .05	p ≤ .001
Only Reward (M = 1.49, SD = .34) (M = 1.33, SD = .26)	p ≤ .001 p ≤ .05	p = .15	N/A	p = .97	p = .99 p = .90	p = .45 p ≤ .001
Only Social (M = 1.51, SD = .34)	p ≤ 10^{-4}	p ≤ .05	p = .97	N/A	p = .99	p = .87
Only Perseveration (M = 1.50, SD = .40) (M = 1.35, SD = .32)	p ≤ 10^{-4} p ≤ .001	p ≤ .05	p = .99 p = .90	p = .99	N/A	p = .71 p ≤ .05
No Sources (M = 1.54, SD = .28) (M = 1.41, SD = .24)	p ≤ 10^{-7} p ≤ 10^{-8}	p ≤ .001	p = .45 p ≤ .001	p = .87	p = .71 p ≤ .05	N/A

The leftmost column of the table above indicates the mean and standard deviation of the reaction times for each decision class. Cells in columns two through seven indicate the significance of Tukey's tests between the decision classes indicated by the row and column. For the leftmost column and comparison cells with two numbers, the upper number corresponds to social conditions where location information was available (Locations and Both conditions), while the lower number indicates the significance of the comparison for social conditions where location information was unavailable (Isolated and Points conditions). Cells with only one number represent comparisons that were only possible for decision classes where location information was available. ANOVA revealed a significant effect of decision class ($F_{3,2372}$ = 7.03, p < 10^{-14}, ω^2 = .03) and a significant effect of location availability ($F_{1,2372}$ = 102.43, p < 10^{-22}, ω^2 = .04), but no interaction between the two factors ($F_{3,2372}$ = .30, p = .82). Separate ANOVA's for each category of location availability revealed main effects of decision class when location information was available ($F_{5,1769}$ = 8.22, p < 10^{-6}, ω^2 = .02) and when location information was unavailable ($F_{3,1769}$ = 12.97, p < 10^{-7}, ω^2 = .03). Post-hoc pairwise comparisons within decisions classes between location-available and location-unavailable social conditions were all significant at p < .01 or less.

Table S3. Statistical data for gaze times across decision classes: participant's points.

	Only Reward	Only Social	Only Perseveration
Only Reward (M = .101, SD = .103) (M = .163, SD = .139)	N/A	p = .89	p = .72 p = .64
Only Social (M = .115, SD = .109)	p = .89	N/A	p = .95
Only Perseveration (M = .111, SD = .111) (M = .160, SD = .144)	p = .72 p = .64	p = .95	N/A

The leftmost column of the table above indicates the mean and standard deviation of the gaze times for each of the three decision classes (expressed as the fraction of the trial spent fixating on the participant's points). Cells in columns two through four indicate the significance of Tukey's tests between the decision classes indicated by the row and column. For the leftmost column and comparison cells with two numbers, the upper number corresponds to social conditions where location information was available (Locations and Both conditions), while the lower number indicates the significance of the comparison for social conditions where location information was unavailable (Isolated and Points conditions). Cells with only one number represent comparisons that were only possible for decision classes where location information was available. ANOVA revealed a significant effect of location availability ($F_{1,696} = 36.7$, $p < 10^{-8}$, $\omega^2 = .05$), but no significant effect of decision class ($F_{1,696} = .67$, $p = .41$) and no interaction between the two factors ($F_{1,696} = .05$, $p = .82$). Separate ANOVA's for each category of location availability revealed no effect of decision class when location information was available ($F_{2,527} = .53$, $p = .59$) or when location information was unavailable ($F_{1,345} = .13$, $p = .72$). Post-hoc pairwise comparisons within decisions classes between location-available and location-unavailable social conditions were all significant at $p < .001$ or less.

Table S4. Statistical data for gaze times across decision classes: other group members' markers.

	Only Reward	Only Social	Only Perseveration
Only Reward (M = .032, SD = .031)	N/A	p = .99	p = .80
Only Social (M = .031, SD = .026)	p = .99	N/A	p = .82
Only Perseveration (M = .029, SD = .028)	p = .80	p = .82	N/A

The leftmost column of the table above indicates the mean and standard deviation of the gaze times for each of the three decision classes (expressed as the fraction of the trial spent fixating on other group members' markers). Cells in columns two through four indicate the significance of Tukey's tests between the decision classes indicated by the row and column. As other group members' markers were only available during the Location and Both conditions, all data correspond to the mean values for those social conditions. ANOVA revealed no significant effect of decision class ($F_{2,527} = 1.04$, p = .35).

Table S5. Neuroimaging analysis: source disagreement [Isolated + Points].

Brain Region	MNI Coordinates	p value	Voxels
L Parietal Lobe	(-27, -44, 28)	$p \leq 10^{-5}$	748
R Parietal Lobe	(41, -31, 32)	$p \leq 10^{-5}$	524
L Middle Frontal Gyrus	(-48, 0, 16)	$p \leq 10^{-5}$	347
R Middle Frontal Gyrus	(27, -10, 48)	$p \leq 10^{-5}$	228
L dlPFC	(-41, 51, 20)	$p \leq 10^{-5}$	109
L Insula	(-31, 17, 8)	$p \leq 10^{-4}$	49
R dlPFC	(41, 44, 32)	$p \leq 10^{-5}$	44
dACC	(-3, 17, 44)	$p \leq 10^{-3}$	15
R Inferior Frontal Gyrus	(54, 10, 16)	$p \leq 10^{-3}$	7

The table above displays the location, size and statistical significance of the regions shown in Figure 7C, top row (which indicates the magnitude of BOLD activity according to the level of disagreement between the reward-based and perseveration-based sources for conditions in which location-based information about other group members was unavailable: the Isolated and Points conditions). Activations are shown for regions surpassing a statistical threshold of $p < .001$ and a cluster size of 5 voxels. L, left hemisphere; R, right hemisphere. Coordinates and statistical values are shown for the voxel of highest significance within each cluster.

Table S6. Neuroimaging analysis: [Locations + Both].

Brain Region	MNI Coordinates	p value	Voxels
L Parietal Lobe	(-61, -31, 40)	$p \leq 10^{-5}$	632
L Middle Frontal Gyrus	(-17, -3, 52)	$p \leq 10^{-5}$	411
L dlPFC	(-44, 48, 16)	$p \leq 10^{-5}$	252
R Middle Frontal Gyrus	(14, 17, 40)	$p \leq 10^{-5}$	233
R dlPFC	(24, 37, 16)	$p \leq 10^{-5}$	203
dACC	(-3, 14, 40)	$p \leq 10^{-5}$	202
L Insula	(-54, 7, 40)	$p \leq 10^{-4}$	135
R Parietal Lobe	(41, -27, 40)	$p \leq 10^{-4}$	73
R Precuneus	(10, -54, 52)	$p \leq 10^{-3}$	17
R Cingulate Gyrus	(17, -34, 44)	$p \leq 10^{-3}$	13
R Putamen	(27, 17, 4)	$p \leq 10^{-3}$	5

The table above displays the location, size and statistical significance of the regions shown in Figure 7C, bottom row (which indicates the magnitude of BOLD activity according to the level of disagreement between the reward-based, socially-based and perseveration-based sources for conditions in which location-based information about other group members was available: the Locations and Both conditions). Activations are shown for regions surpassing a statistical threshold of p < .001 and a cluster size of 5 voxels. L, left hemisphere; R, right hemisphere. Coordinates and statistical values are shown for the voxel of highest significance within each cluster.

Table S7. Neuroimaging analysis: correlations with reward Ratio R

Brain Region	MNI Coordinates	p value	Voxels
Midbrain	(7, -14, -12)	$p \leq 10^{-5}$	295
L Putamen	(-27, -24, 4)	$p \leq 10^{-4}$	45
Cuneus	(10, -78, 4)	$p \leq 10^{-6}$	39
Posterior Cingulate Gyrus	(3, -20, 24)	$p \leq 10^{-4}$	14
R Thalamus	(24, -20, -4)	$p \leq 10^{-3}$	7

The table above displays the location, size and statistical significance of the regions shown in Figure S8A: regions whose activity was positively correlated with the input to the reward-based component: the reward ratio R. Activations are shown for regions surpassing a corrected statistical threshold of $p < .001$ and a cluster size of 5 voxels. L, left hemisphere; R, right hemisphere. Coordinates and statistical values are shown for the voxel of highest significance within each cluster.

Table S8. Neuroimaging analysis: correlation with group centroid angle θ.

Brain Region	MNI Coordinates	p value	Voxels
L Middle Frontal Gyrus	(-24, -7, 48)	$p \leq 10^{-4}$	112
L Postcentral Gyrus	(-31, -37, 32)	$p \leq 10^{-4}$	80
R Middle Frontal Gyrus	(7, 10, 52)	$p \leq 10^{-4}$	45
R Thalamus	(3, -3, 12)	$p \leq 10^{-3}$	10
R Caudate	(17, -3, 20)	$p \leq 10^{-3}$	9
R Parietal Lobe	(-34, -58, 60)	$p \leq 10^{-3}$	9
Midbrain	(0, -34, -12)	$p \leq 10^{-3}$	9

The table above displays the location, size and statistical significance of the regions shown in Figure S8B: regions whose activity was positively correlated with the input to the socially-based component: the group centroid angle θ. Activations are shown for regions surpassing a corrected statistical threshold of p < .001 and a cluster size of 5 voxels. L, left hemisphere; R, right hemisphere. Coordinates and statistical values are shown for the voxel of highest significance within each cluster.

Table S9. Neuroimaging analysis: correlation with consecutive actions N.

Brain Region	MNI Coordinates	p value	Voxels
vmPFC	(-3, 37, -4)	$p \leq 10^{-4}$	50

The table above displays the location, size and statistical significance of the regions shown in Figure S8C: regions whose activity was positively correlated with the input to the perseveration-based component: the number of consecutively repeated actions N. Activations are shown for regions surpassing a corrected statistical threshold of p < .001 and a cluster size of 5 voxels. Coordinates and statistical values are shown for the voxel of highest significance within each cluster.

Table S10. Statistical comparisons of mean vmPFC activity across number of disagreeing sources.

	0 disagreeing Sources	1 disagreeing source	2 disagreeing sources	3 disagreeing Sources
0 disagreeing sources (M = -.034, SD = .444) (M = .013, SD = .218)	N/A	p = .99 p = .24	p = .97 p ≤ .005	p = .41
1 disagreeing source (M = -.034, SD = .196) (M = -.034, SD = .123)	p = .99 p = .24	N/A	p = .96 p = .17	p = .34
2 disagreeing sources (M = -.057, SD = .151) (M = -.085, SD = .117)	p = .97 p ≤ .005	p = .96 p = .17	N/A	p = .66
3 disagreeing sources (M = -.109, SD = .150)	p = .41	p = .34	p = .66	N/A

The leftmost column of the table above indicates the mean and standard deviation of the BOLD signal in the vmPFC region of interest (ROI) for each level of disagreement between reward-based, socially-based, and perseveration-based sources (expressed as z-scores). Cells in columns two through five indicate the significance of Tukey's tests between the disagreement levels indicated by the row and column. For the leftmost column and comparison cells with two numbers, the upper number corresponds to social conditions where location information was available (Locations and Both conditions), while the lower number corresponds social conditions where location information was unavailable (Isolated and Points conditions). Cells with only one number represent comparisons that were only possible for levels of disagreement where location information was available. A joint analysis pooling data for which locations of other group members were available and unavailable revealed no effect of source disagreement, location availability, or interaction (respectively, $F_{2,339} = 2.15$, $p = .12$; $F_{1,339} = .07$, $p = .79$; $F_{2,339} = .79$, $p = .46$). There was also no effect of source disagreement in a separate analysis of trials for which location-based information was available ($F_{3,225} = 5.72$, $p = .31$). There *was* an effect of source disagreement on trials for which location-based information was unavailable ($F_{2,175} = 5.72$, $p < .005$, $\omega^2 = .05$); however, the pattern of activity exhibited by the vmPFC *was the opposite to that shown in Figure 7*: vmPFC activity was *lower* for trials in which there was more disagreement between sources.